The dynamics of COVID-19 in the UAE based on fractional derivative modeling using Riesz wavelets simulation

Mutaz Mohammad[*], *Alexander Trounev*[†], *Carlo Cattani*[‡]

Abstract

The well-known novel virus (COVID-19) is a new strain of coronavirus which considered by the World Health Organization (WHO) as a dangerous epidemic. More than 3.5 million positive cases and 250 thousand deaths (up to May 5, 2020) caused by COVID-19 and has affected more than 280 countries over the world. Therefore, studying the prediction of this virus spreading in further attracts a major public attention. In the United Arab Emirates (UAE), up to same date, there are 14730 positive cases and 137 deaths according to national authorities. In this work, we study a dynamical model based on fractional derivative of nonlinear equations that describe the outbreak of COVID-19 according to the available infection data announced and approved by the national committee in the press. We simulate the available total cases reported based on Riesz wavelets generated by some refinable functions, namely the smoothed pseudo-splines of type I and II with high vanishing moments. Based on these data, we also consider the formulation of the pandemic model using Caputo fractional derivative definition. We then solve numerically the nonlinear system that describe the dynamics of COVID-19 with the given resources based on the collocation Riesz wavelet system constructed. We present graphical illustrations of the numerical solutions of all parameter of the model being handled under different situations. It is anticipated that these results will contribute to the ongoing research to reduce the spreading of the virus and infection cases.

Keywords: Fractional differential equations; novel coronavirus; Reisz wavelet system; smoothed pseudo-splines; mathematical model.

1 Introduction

In March 2020, WHO has announced the novel corona-virus as a pandemic after the outbreak on the end of January 2020, where it was declared a public health emergency for the global. Since then, the pandemic has affected almost all countries around the world and kills more than 290,000 of people worldwide. The virus can easily spreads from one to another and no treatment or vaccine can do the needs [1, 2]. Even though a vaccine could be more than a year away, doctors are experimenting with drugs and therapies to help ease the virus symptoms/spreading.

Given the dangerous situation, many researchers started working on formulating models that best describe the dynamics of all possible parameters responsible for the daily cases reported including deaths, control the fatality rate, and prediction of COVID-19 behavior in future within a specific region. It is known that several models can describe the same system, which is a challenging step.

[*]Zayed University (Corresponding: Mutaz.Mohammad@zu.ac.ae).
[†]Kuban State Agrarian University
[‡]Engineering School, University of Tuscia

However, in this paper we used the well-known parsimony principle, where the model should be constructed in a simple way as possible but also with complexity when needed.

Fractional derivatives have been proven as a useful tool in a wide area of applications in science and engineering [3–9], including customary in groundwater analysis, the modeling of infection disease, and epidemic systems to discover and predict the spreading of many diseases. It is known that Covid-19 originated in Bats and infect humans and can infect several animals such as cats and ferret. There is no case (up to date) of direct transmission from bat to human, but yet a proposal says there is a host-reservoir most likely involved between them. We consider the model presented in [10] developed based on

$$Bats \Rightarrow Hosts \Rightarrow Reservoir \Rightarrow People$$

formulation setting that used Atangana-Baleanu fractional derivative sense. In this paper, we use the Caputo fractional derivative definition to study the the model. The advantage of using such definition is that it allows traditional and various types of ICs to be consider in the creation of the dynamical model. Wavelets appear in a variety of advanced applications such as filter banks constructions arise in image processing. This is largely due to the fact that wavelets have the right structure to capture the sparsity in 'physical' images, perfect mathematical properties such as its multi-scale structure, sparsity, smoothness, compactly supported, and high vanish moments. It has many applications in fractional integral and differential equations (see for example [11–21].

Riesz wavelets in $L_2(\mathbb{R})$ have been used extensively in the context of both pure and numerical analysis in many applications, due to their well prevailing and recognized theory and its natural properties such as sparsity and stability which lead to a well-conditioned scheme. In this paper, an effective and accurate technique based on Riesz wavelets is presented for solving the transmission model of COVID-19 based on Caputo fractional derivative. The advantage of using such wavelets, lies on its simple structure of the reduced systems and in the powerfulness of obtaining approximated solutions for such equations that have weakly singular kernels. The proposed method shows a good performance and high accuracy orders.

Let us recall some definitions and notation needed for this paper. A function $\phi \in L_2(\mathbb{R})$ is called refinable if

$$\phi = \sum_{k\mathbb{Z}} a[k]\phi(2\cdot - k), \tag{1.1}$$

where $a[k] \in \ell_2(\mathbb{Z})$ is finitely supported sequence and is called the refinement mask of ϕ. The corresponding wavelet function is defined by

$$\psi = \sum_{k\mathbb{Z}} b[k]\phi(2\cdot - k), \tag{1.2}$$

where $b[k] \in \ell_2(\mathbb{Z})$ is finitely supported sequence and is called the high pass filter of ψ.

In this paper, for $f \in L_1(\mathbb{R})$ (which can be extended to $L_2(\mathbb{R})$), we use the following Fourier transform defined by

$$\hat{f}(\xi) = \frac{1}{\sqrt{2\pi}} \int_{\mathbb{R}} e^{-ix\xi} f(x)dx.$$

The Fourier series of the sequence a is defined by

$$\hat{a}(\xi) = \sum_{k\in\mathbb{Z}} a[k]e^{-ik\xi}, \quad \xi \in \mathbb{R}. \tag{1.3}$$

Pseudo-splines have attracted many researcher due to their significant contribution to both numerical computations and analysis. The constructions of pseudo-splines tracked back to the well known work produced by Daubechies et. al. in [22, 23], It is a family of refinable functions with compact support and have extensive flexibility in wavelets and applications. Pseudo-splines known as a generalization of many well-known refinable functions such as the B-splines, interpolate and orthonormal refinable functions [24]. We refer the reader to [22, 23, 25–29] and references therein for more details.

2 Riesz wavelets via smoothed pseudo-splines

We use the smoothed pseudo-splines introduced in [29] to construct Riesz wavelets and use it to apply our numerical scheme for solving different types of FIDEs. Pseudo-splines of order (p,q) of type I and II, ${}_k\phi_{(p,q)}, k=1,2$, are defined in terms of their refinement masks, where

$$|{}_1\hat{a}_{(p,q)}(\xi)|^2 = \sum_{m=0}^{q} \binom{p+q}{m} (\cos(\xi/2))^{2(p+q-m)} \sin^{2m}(\xi/2)$$

and

$${}_2\hat{a}_{(p,q)}(\xi) = |{}_1\hat{a}_{(p,q)}(\xi)|^2.$$

Note that, the refinement mask of the pseudo-splines of type I with order (p,q) is obtained using Fejér-Riesz Theorem. The refinable pseudo-spline function generated using the above refinment masks is defined by

$${}_k\hat{\phi}_{(p,q)}(\cdot) = \prod_{m=1}^{\infty} {}_k\hat{a}_{(p,q)}(\cdot/2^m), \quad k=1,2. \tag{2.1}$$

They are two types of smoothed pseudo-splines defined by its refinable masks. For $r \geq p$, we have the smoothed refinable pseudo-splines of type I ($k=1$), and II ($k=2$) with order (r,p,q), such that

$${}_k\phi_{(r,p,q)}(\cdot) = {}_k\phi_{p,q} * \chi^{r-p}_{[-\frac{1}{2},\frac{1}{2}]}(\cdot), \quad k=1,2, \tag{2.2}$$

where

$$\chi^{r-p}_{[-\frac{1}{2},\frac{1}{2}]}(\cdot) = \chi_{[-\frac{1}{2},\frac{1}{2}]} * \cdots * \chi_{[-\frac{1}{2},\frac{1}{2}]}, \text{ for } (r-p) \text{ times},$$

where χ_A is the indicator function on the set A. Similarly, the refinement masks of both types of ${}_k\phi_{(r,p,q)}$, for $k=1,2$, respectively are given by

$$|{}_1\hat{a}_{(r,p,q)}(\xi)|^2 = \sum_{m=0}^{q} \binom{p+q}{m} (\cos(\xi/2))^{2(r+q-m)} \sin^{2m}(\xi/2)$$

and for $r \geq 2p$,

$${}_2\hat{a}_{(r,p,q)}(\xi) = \sum_{m=0}^{q} \binom{p+q}{m} (\cos(\xi/2))^{2q+r-p} \sin^{2m}(\xi/2)$$

Riesz wavelets have been studies extensively in the literature, for example see [**?**, **?**, **?**, **?**] and other references.

Definition 2.1. *We say that the set* $\mathcal{M}(\psi^\ell) = \left\{\psi^\ell_{j,k} = 2^{j/2}\psi^\ell(2^j\cdot - k), \ell = 1,\dots,N\right\}, \psi^\ell \in L_2(\mathbb{R})$ *generate a Riesz wavelet in* $L_2(\mathbb{R})$ *if for any finitely supported sequence* $\left\{n^\ell_{j,k}, \ell = 1,\dots,N; j,k \in \mathbb{Z}\right\}$ *there exist positive numbers* c *and* C *such that*

$$c\sum_{\ell=1}^{N}\sum_{j\in\mathbb{Z}}\sum_{k\in\mathbb{Z}} |n^\ell_{j,k}|^2 \leq \left\|\sum_{\ell=1}^{N}\sum_{j\in\mathbb{Z}}\sum_{k\in\mathbb{Z}} n^\ell_{j,k}\psi^\ell_{j,k}\right\|^2 \leq C\sum_{\ell=1}^{N}\sum_{j\in\mathbb{Z}}\sum_{k\in\mathbb{Z}} |n^\ell_{j,k}|^2, \ \forall g \in L_2(\mathbb{R}), \tag{2.3}$$

where

$$\|g\|^2 = \langle g, g\rangle, \text{ and } \langle f, g\rangle = \int_{\mathbb{R}} f(x)\overline{g(x)}dx.$$

If $\mathcal{M}$ defined in Definition 2.1 is a Riesz wavelets for $L_2(\mathbb{R})$, then we can conclude the following expansion for any function $f \in L_2(\mathbb{R})$ such that

$$f = \sum_{\ell=1}^{N} \sum_{j,k\in\mathbb{Z}} \langle f, \psi_{j,k}^{\ell} \rangle \, \psi_{j,k}^{\ell}. \tag{2.4}$$

Equation 2.4 can be truncated by

$$\mathcal{V}_M f = \sum_{\ell=1}^{N} \sum_{j\le M-1} \sum_{k\in\mathbb{Z}} \langle f, \psi_{j,k}^{\ell} \rangle \, \psi_{j,k}^{\ell}. \tag{2.5}$$

Lets provide some examples of Riesz wavelet systems and explicit expression of thier filter banks

Example 2.1. For $(r, p, q) = (6, 2, 1)$, we have the following refinable masks:

$$\begin{aligned} {}_1\hat{a}_{(6,2,1)}(\xi) &= \frac{1}{2}\left(\sqrt{3}+1\right) e^{-\frac{1}{2}5i\xi} \left(1 + \left(\sqrt{3}-2\right) e^{i\xi}\right) \cos^3\left(\frac{\xi}{2}\right), \\ {}_1\hat{b}_{(6,2,1)}(\xi) &= e^{-i\xi}\, \overline{{}_1\hat{a}_{(6,2,1)}(\xi+\pi)}, \end{aligned}$$

where

$$\begin{aligned} {}_1\phi_{(6,2,1)}(2\cdot) &= {}_1\hat{a}_{(6,2,1)}(\cdot)\,{}_1\phi_{(6,2,1)}(\cdot), \\ {}_1\psi_{(6,2,1)}(2\cdot) &= {}_1\hat{b}_{(6,2,1)}(\cdot)\,{}_1\phi_{(6,2,1)}(\cdot). \end{aligned}$$

Then, $\mathcal{M}({}_1\psi_{(6,2,1)})$ forms Riesz wavelet systems for $L_2(\mathbb{R})$. Note that the vanishing moments for the system systems is 6.

Example 2.2. For $(r, p, q) = (9, 3, 2)$, we have the following refinable masks:

$$\begin{aligned} {}_2\hat{a}_{(9,3,2)}(\xi) &= \frac{1}{4}\cos^{10}\left(\frac{\xi}{2}\right)(-156\cos(\xi) + 33\cos(2\xi) + 127), \\ {}_2\hat{b}_{(9,3,2)}(\xi) &= e^{-i\xi}\, \overline{{}_2\hat{a}_{(9,3,2)}(\xi+\pi)}, \end{aligned}$$

where ${}_1\hat{a}_{(9,3,2)}(\xi)$ is obtained using Fejér-Riesz factorization theorem, so

$$|{}_1\hat{a}_{(9,3,2)}(\xi)|^2 \approx {}_2\hat{a}_{(9,3,2)}(\xi),$$

and that where

$$\begin{aligned} {}_2\phi_{(9,3,2)}(2\cdot) &= {}_1\hat{a}_{(9,3,2)}(\cdot)\,{}_1\phi_{(9,3,2)}(\cdot), \\ {}_2\psi_{(9,3,2)}(2\cdot) &= {}_1\hat{b}_{(9,3,2)}(\cdot)\,{}_1\phi_{(9,3,2)}(\cdot). \end{aligned}$$

Here we found ${}_1\hat{a}_{(9,3,2)}(\xi)$ numerically, see Figure 1. Note that

$$\left||{}_1\hat{a}_{(9,3,2)}(\xi)|^2 - {}_2\hat{a}_{(9,3,2)}(\xi)\right| \le \mathcal{O}(10^{-13}).$$

Then, $\mathcal{M}({}_2\psi_{(9,3,2)})$ forms Riesz wavelet systems for $L_2(\mathbb{R})$.

Definition 2.2. *For a real function $u(t)$ where $t, \alpha > 0$, and $n \in \mathbb{N}$,*

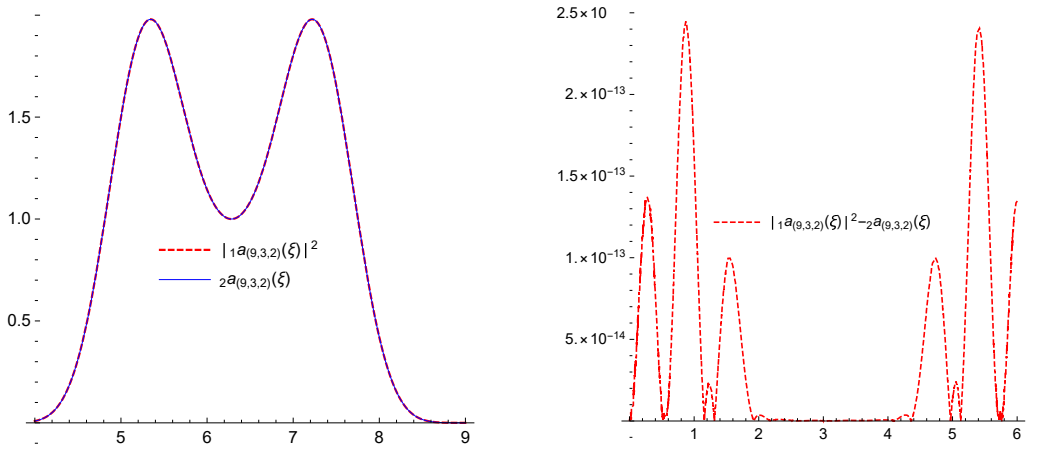

Fig. 1: The graphs of the masks $\left|{}_1\hat{a}_{(9,3,2)}(\xi)\right|^2$, ${}_2\hat{a}_{(9,3,2)}(\xi)$ and its difference in Example 2.2.

- *The Caputo's fractional derivative CFD,*

$$\mathcal{D}_*^{\alpha}u(t)=\frac{1}{\Gamma(n-\alpha)}\int_0^t\frac{u^{(n)}(x)}{(t-x)^{\alpha+1-n}}dx,\ n-1<\alpha\leq n.$$

- *The Reimann-Liouville fractional integral operator (R-LFI),*

$$\mathcal{I}^{\alpha}u(t)=\frac{1}{\Gamma(\alpha)}\int_0^t\frac{u(x)}{(t-x)^{1-\alpha}}dx,\ \textit{and}\ n-1<\alpha\leq n.$$

formulation

3 Transmission model and Numerical algorithm based on Riesz wavelet fitting

The original data is fitted by a set of discrete Riesz wavelet coefficients, where features can be extracted from these coefficients. The simulated data based on the Riesz wavelet systems is illustrated in Figure 2.

We consider the following new modified transmission model that obtained by changing the left hand side of the system presented in [10] by changing the operator

$${}_a^{ABC}\mathcal{D}_t^{\alpha}u(t)\ to\ \mathcal{D}_t^{\alpha}u(t)$$

for all unknown functions $S_p, E_p, I_p, A_p, R_p, M$, where ρ represent the fractional order parameter. Note that the system is subject to non-negative initial conditions. So the new system is defined as follows:

$$\begin{aligned}
\mathcal{D}_t^{\alpha}S_p(t) &= \Pi_p-\mu_pS_p-\frac{\eta_pS_p(I_p+\psi A_p)}{N_p}-\eta_wS_pM &(3.1)\\
\mathcal{D}_t^{\alpha}E_p(t) &= \frac{\eta_pS_p(I_p+\psi_pA_p)}{N_p}+\eta_wS_pM-(1-\theta_p)\omega_pE_p-\theta_p\alpha &(3.2)\\
\mathcal{D}_t^{\alpha}I_p(t) &= (1-\theta_p)\omega_pE_p-(\tau_p+\mu_p)I_p &(3.3)\\
\mathcal{D}_t^{\alpha}A_p(t) &= \theta_p\rho_pE_p-(\tau_{ap}+\mu_p)A_p &(3.4)\\
\mathcal{D}_t^{\alpha}R_p(t) &= \tau_pI_p+\tau_{ap}A_p-\mu_pR_p &(3.5)\\
\mathcal{D}_t^{\alpha}M(t) &= \varrho_pI_p+\varpi_pA_p-\pi M &(3.6)
\end{aligned}$$

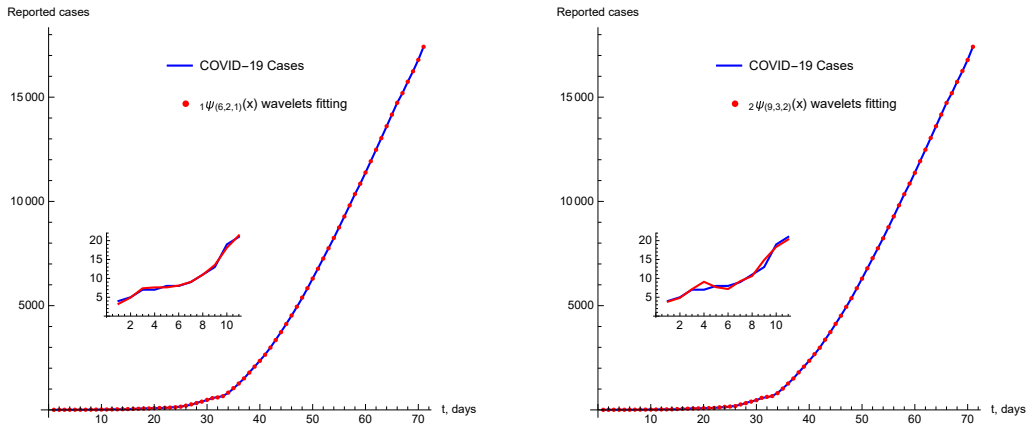

Fig. 2: Reported cases of COVID-19 in the UAE with the Riesz wavelet fitting based on Examples 2.1 and 2.2, respectively .

given the model parameters and its values in Table 1: It is reasonable to consider this model with

Tab. 1: Parameters description and estimated-fitted values given $\rho = 0.9$

Parameter	Description	Parameter value
$S_p(t)$	The susceptible cases	–
$E_p(t)$	The exposed cases	–
$I_p(t)$	The infected cases	–
$A_p(t)$	The asymptotically cases	–
$R_p(t)$	The recovered cases	–
$M(t)$	The infected cases	–
Π_p	Birth rate	341.706
μ_p	Natural mortality rate	0.0000353513
η_p	Contact rate	0.01
ψ_p	Transmissibility multiple	0.01
η_w	Disease transmission coefficient	0.000001
θ_p	The proportion of asymptomatic infection	0.09
ω_p	Incubation period (bats)	0.00039
ρ_p	Incubation period (hosts)	0.001
τ_p	recovery rate of I_p	0.1593
τ_{ab}	recovery rate of A_p	0.95
ϱ_p	Contribution of the virus to M by I_p	0.0001
ϖ_p	Contribution of the virus to M by A_p	0.00089
π	Removing rate of virus from M	0.009

proper changes as it is formulated based on the resources and cases detected in Wuhan-China. The cases spread to more than 280 countries around the world, so some parameters values will be considered in the current study. For more details about the formulation and stability results, we refer to the reference **??**. To illustrate the fitting, we use some examples of Riesz wavelet systems to be used in the data fitting using the discrete Riesz wavelet transform defined in (1.3) based on different types of smoothed pseudo-splines of order I and II.

We provide a numerical algorithm based on the collocation method by discretize the domain

function across the Riesz wavelet system being used to solve the model. The system is generated using the smoothed pseudo-splines of type I and II with different orders. The model defined in Equations (3.1)-(3.5) can be reduced as below:

$$\begin{aligned}
\frac{1}{\Gamma(1-\alpha)}\int_0^t \frac{S_p'(x)}{(t-x)^\alpha}dx &= \Pi_p - \mu_p S_p - \frac{\eta_p S_p(I_p+\psi A_p)}{N_p} - \eta_w S_p M \\
\frac{1}{\Gamma(1-\alpha)}\int_0^t \frac{E_p'(x)}{(t-x)^\alpha}dx &= \frac{\eta_p S_p(I_p+\psi A_p)}{N_p} + \eta_w S_p M - (1-\theta_p)\omega_p E_p - \theta_p\rho_p E_p \\
\frac{1}{\Gamma(1-\alpha)}\int_0^t \frac{I_p'(x)}{(t-x)^\alpha}dx &= (1-\theta_p)\omega_p E_p - (\tau_p+\mu_p) I_p \\
\frac{1}{\Gamma(1-\alpha)}\int_0^t \frac{A_p'(x)}{(t-x)^\alpha}dx &= \theta_p\rho_p E_p - (\tau_{ap}+\mu_p) A_p \\
\frac{1}{\Gamma(1-\alpha)}\int_0^t \frac{R_p'(x)}{(t-x)^\alpha}dx &= \tau_p I_p + \tau_{ap} A_p - \mu_p R_p \\
\frac{1}{\Gamma(1-\alpha)}\int_0^t \frac{M'(x)}{(t-x)^\alpha}dx &= \varrho_p I_p + \varpi_p A_p - \pi M.
\end{aligned}$$

Using collocation method based on the nodes $t_i, i \in \mathbb{N}$ in the above equations, we obtain the following equations that generate a system of nonlinear equations to be solved numerically:

$$\begin{aligned}
-\mathcal{D}_t^\alpha S_p(t_i) + \Pi_p - \mu_p S_p(t_i) &- \frac{\eta_p S_p(t_i)(I_p(t_i)+\psi A_p(t_i))}{N_p} - \eta_w S_p(t_i) M(t_i) = 0 \\
-\mathcal{D}_t^\alpha E_p(t_i) + \frac{\eta_p S_p(t_i)(I_p(t_i)+\psi A_p(t_i))}{N_p} &+ \eta_w S_p(t_i) M(t_i) - (1-\theta_p)\omega_p E_p(t_i) - \theta_p\rho_p E_p(t_i) = 0 \\
-\mathcal{D}_t^\alpha I_p(t_i) &+ (1-\theta_p)\omega_p E_p(t_i) - (\tau_p+\mu_p) I_p(t_i) = 0 \\
-\mathcal{D}_t^\alpha A_p(t_i) &+ \theta_p\rho_p E_p(t_i) - (\tau_{ap}+\mu_p) A_p(t_i) = 0 \\
-\mathcal{D}_t^\alpha R_p(t_i) &+ \tau_p I_p(t_i) + \tau_{ap} A_p(t_i) - \mu_p R_p(t_i) = 0 \\
-\mathcal{D}_t^\alpha M(t_i) &+ \varrho_p I_p(t_i) + \varpi_p A_p(t_i) - \pi M(t_i) = 0.
\end{aligned}$$

The parameters value listed in Table 1 were estimated based on some known results and assumptions, it is taken into consideration the effect of each sub-group/population in the virus spread. Based on official data on the COVID-19 in the UAE among the residents, the estimation on the parameters of the dynamic of the virus will be considered. This due to the fact that the dynamic of the virus transmission from country (e.g. the case study UAE) to another (China) does not change much. In addition, the other parameters are relating to the structure of populations and has no affect on the nature of the virus.

The total population, $N(0)$, of the UAE in 2019 is approximately 9.666 millions. The life expectancy in the UAE for the year of 2019 is 77.5. Therefore, the the natural mortality rate is $1/(77.5 \times 365)$. The birth rate is estimated by multiplying the value of total population times the mortality rate, so it is estimated by the value 341.706. For the initial values of the model, we consider the population size 9.666 millions for $t = 0$. It is assumed that the number of infected people was 300 there was no recovered cases initially, and $R_p(0) = 0$. Hence, we have the following ICs:

$$S_p(0) = \frac{9344440}{N_p(0)}, A_p(0) = \frac{200}{N_p(0)}, E_p(0) = \frac{321060}{N_p(0)}, M(0) = \frac{5000}{N_p(0)}.$$

Now, we illustrate some graphical illustrations based on the given parameter vales and simulating the model given via Equations (3.1)-(3.5). The dynamics of COVID-19 based on different values of α

is depicted in Figure 3. In Figure 4, 5 and 5 we provide illustrations for the stability of the model equilibrium by changing ICs, and we numerically calculate the parameters model by considering various ICs of S_p, M, and E respectively.

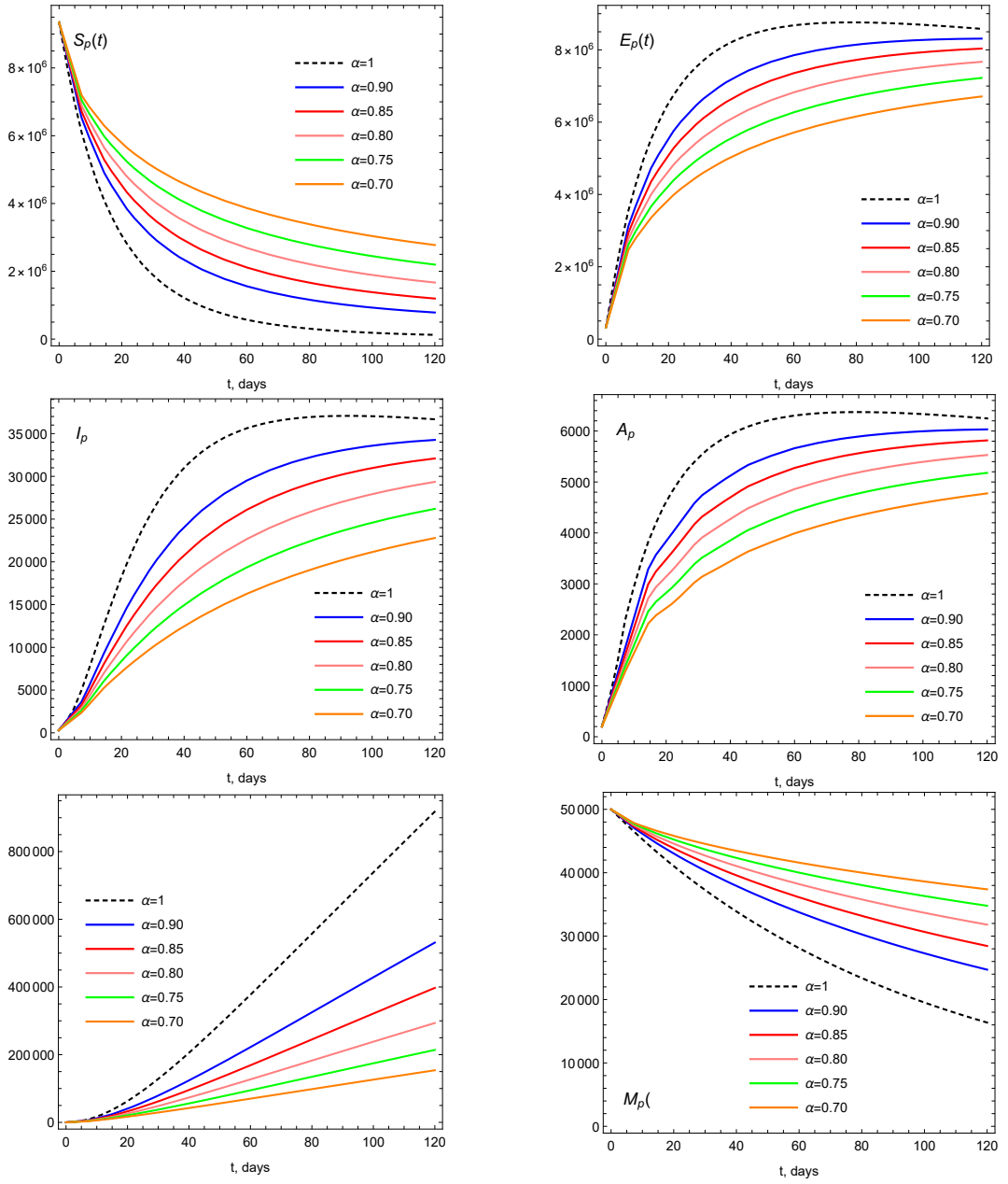

Fig. 3: Illustrations of the dynamics of the model parameters using various values of α

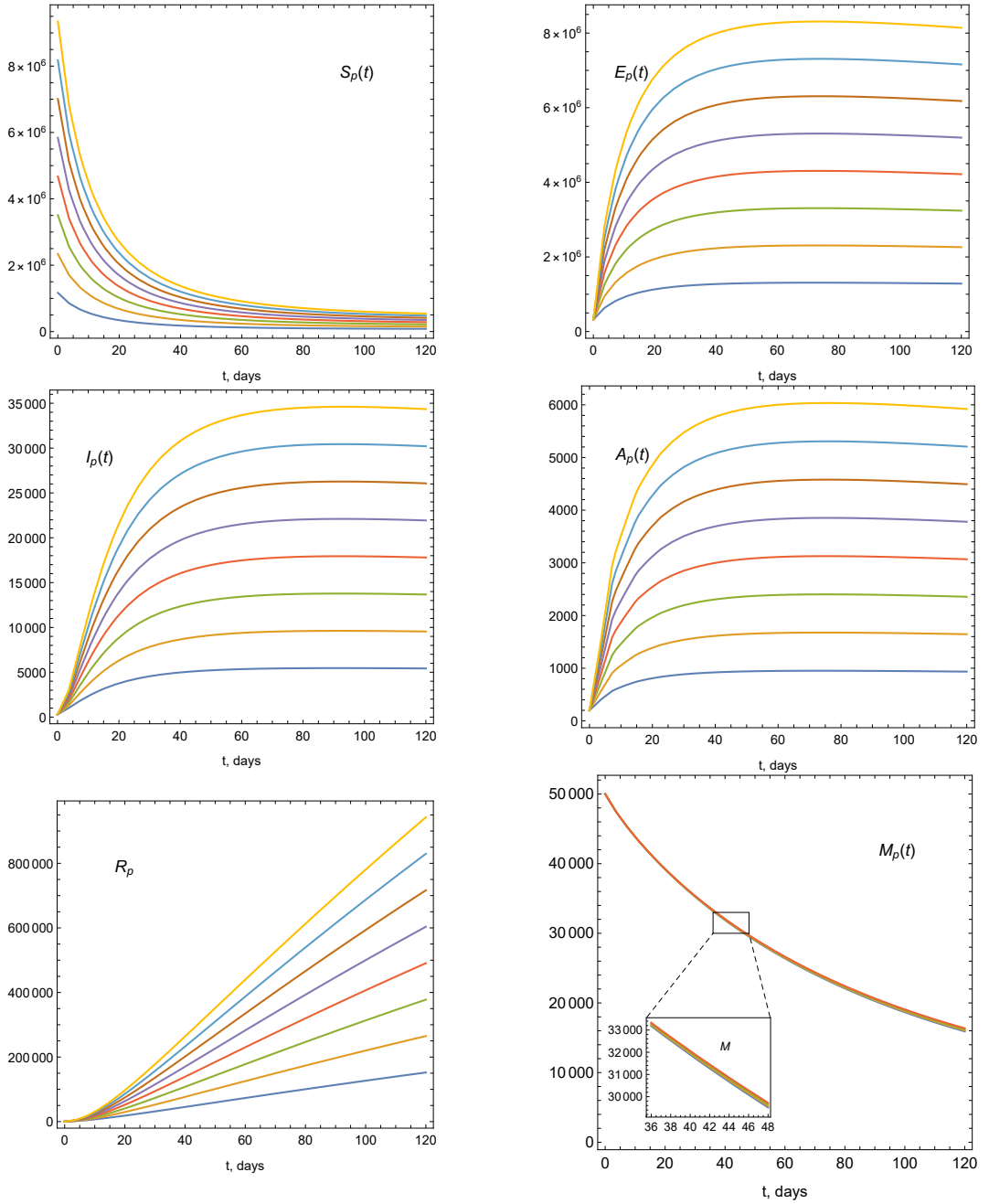

Fig. 4: Illustrations of the dynamics of the model parameters using various ICs

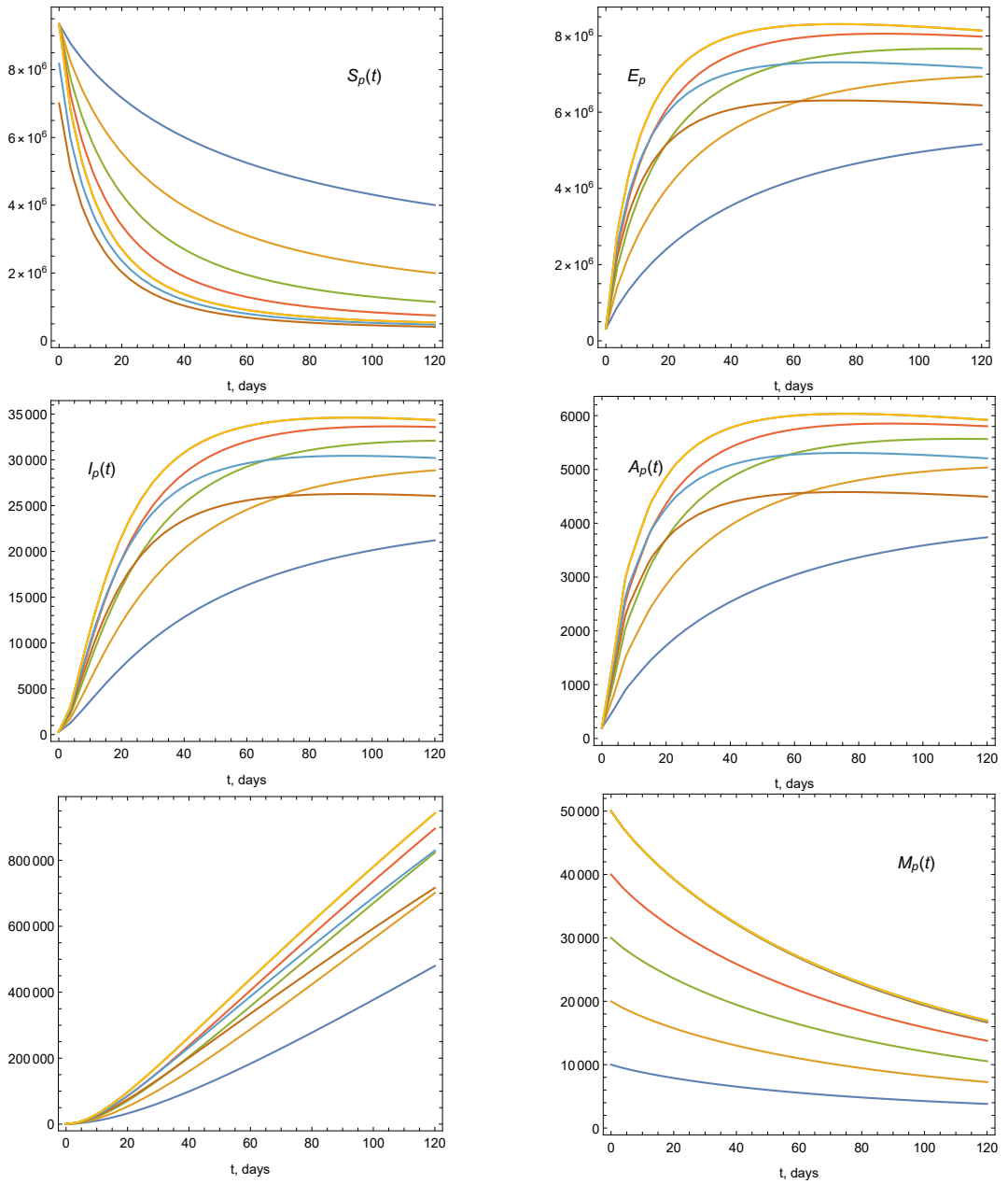

Fig. 5: Illustrations of the dynamics of the model parameters using various ICs

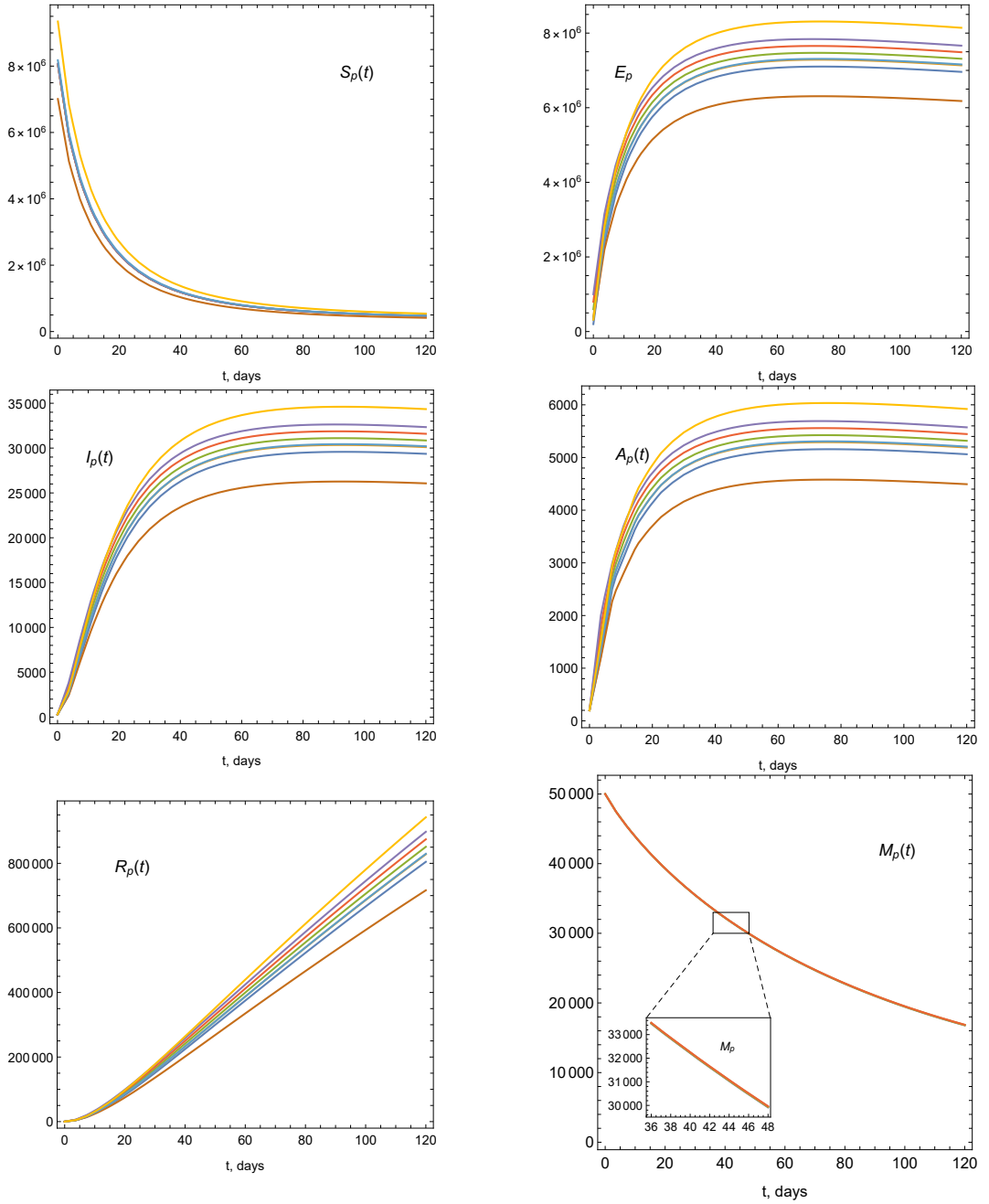

Fig. 6: Illustrations of the dynamics of the model parameters using various ICs

4 Conclusion

In this paper, we considered a fractional model of COVID-19 that describe the virus dynamics based on the resources and announced cases in the UAE. We simulated the original data and fitting it using a new family of Riesz wavelets based on refinable functions that have excellent properties such as symmetries and compact support. The fitting was very accurate compared to the original data. We also used these families to solve the model formulated from nonlinear equations with fractional order. The model used Caputo fractional derivative to best describing the dynamics of the pandemic. We also provided graphical illustrations of the model parameters considering different values of fractional order and various ICs. It turns out that decreasing the order resulting a decrease the infection rates. We intended to consider the model with more data resources to better view of the dynamic and virus spreading in the country.

The research will be extended to include various parameters and aspects in future., specifically to predict the virus and positive cases under fitting the data with quarantine and stem cells factors.

Availability of data and materials
Not applicable.

Competing interests
The authors declare that they have no competing interests.

Funding
Zayed University STG064.

Authors' contributions
The authors declare that the study was realized in collaboration with a distribution of responsibility.

Acknowledgments
The first author would like to thank Zayed University for funding this project under the agreement number STG064.

References

[1] Wuhan, ChinaPopulation1950-2020, ¡https://www.macrotrends.net/cities/20712/wuhan/population¿.

[2] Is the World Ready for the Coronavirus?. Editorial. The New York Times. 29 January 2020. Archived from the original on 30 January 2020.

[3] B. Ghanbari, A. Atangana, A new application of fractional Atangana–Baleanu derivatives: Designing ABC-fractional masks in image processing, Physica A: Statistical Mechanics and its Applications 542 (2020), 123516.

[4] A. Atangana, E. Bonyah, A. Elsadany, A fractional order optimal 4D chaotic financial model with Mittag-Leffler law, Chinese Journal of Physics 65 (2020), 38-53.

[5] A. Atangana, J. Aguilar, M. Kolade, J. Hristov, Fractional differential and integral operators with non-singular and non-local kernel with application to nonlinear dynamical systems, Chaos, Solitons & Fractals 132 (2020) 109493 https://doi.org/10.1016/j.chaos.2019.109493.

[6] A. Atangana, D. Baleanu, New fractional derivatives with nonlocal and non-singular kernel: Theory and application to heat transfer model, Thermal Science, 20 (2016), 763-769.

[7] A. Atangana, I. Koca, Chaos in a simple nonlinear system with Atangana–Baleanu derivatives with fractional order, Chaos, Solitons & Fractals 89 (2016), 447-454.

[8] A. Atangana, On the new fractional derivative and application to nonlinear Fisher's reaction–diffusion equation, Applied Mathematics and Computation 273 (2016), 948-956.

[9] A. Atangana, J. Aguilar, Decolonisation of fractional calculus rules: breaking commutativity and associativity to capture more natural phenomena, the European Physical Journal Plus, 133 (2018), 166.

[10] M. A. Khan, A Atangana, Modeling the dynamics of novel coronavirus (2019-nCov) with fractional derivative, 2020, in press.

[11] M. Mohammad, E. B. Lin, Gibbs phenomenon in tight framelet expansions, Communications in Nonlinear Science and Numerical Simulation, vol. 55, (2018), 84-92.

[12] M. Mohammad, E. B. Lin, Gibbs Effects Using Daubechies and Coiflet Tight Framelet Systems, Contemporary Mathematics, AMS, vol. 706, (2018), 271-282.

[13] M. Mohammad, Special B-spline Tight Framelet and It's Applications, Journal of Advances in Mathematics and Computer Science, 29 (2018): 1-18.

[14] M. Mohammad, On the Gibbs Effect Based on the Quasi-Affine Dual Tight Framelets System Generated Using the Mixed Oblique Extension Principle, Mathematics, 7 (2019).

[15] M. Mohammad, F Howari, G Acbas, Y Nazzal, F AlAydaroos, Wavelets Based Simulation and Visualization Approach for Unmixing of Hyperspectral Data, International Journal of Earth Environmental Sciences 3 (2018).

[16] M. Mohammad, Biorthogonal-Wavelet-Based Method for Numerical Solution of Volterra Integral Equations M Mohammad, Entropy 21 (2019), 1098.

[17] M. Mohammad, A Numerical Solution of Fredholm Integral Equations of the Second Kind Based on Tight Framelets Generated by the Oblique Extension Principle, Symmetry 11 (2019) 854.

[18] M. Mohammad, C. Cattani, A collocation method via the quasi-affine biorthogonal systems for solving weakly singular type of Volterra-Fredholm integral equations, Alex. Eng. J. (2020) In press.

[19] M. Mohammad 2020 J. Phys.: Conf. Ser. 1489 012009.

[20] M. Mohammad, C. Cattani, Applications of bi-framelet systems for solving fractional order differential equations, Fractals, doi:10.1142/S0218348X20400514.

[21] M. Mohammad, 2020 J. Phys.: Conf. Ser. 1489 012009

[22] I. Daubechies, B. Han, A. Ron, Z. Shen, Framelets: MRA-based constructions of wavelet frames, applied and computational harmonic analysis, 14 (2003), Pages 1-46.

[23] I. Selesnick, Smooth wavelet tight frames with zero moments, applied and computational harmonic analysis, 10 (2001), pages 163-181.

[24] B. Han, M. Michelle, Construction of wavelets and framelets on a bounded interval, Analysis and Applications, 16 (2018), 807-849.

[25] B. Dong, Z. Shen, Pseudo-spline, wavelets and framelets, applied and computational harmonic analysis, 22 (2007), pages 78-104.

[26] S. Li, Y. Shen, Pseudo box splines, applied and computational harmonic analysis, 26 (2008), pages 344-356. Dong, B, Shen, Z: Construction of biorthogonal wavelets from pseudo-splines. Journal of Approximation Theory, 138 (2006), pages 211-231.

[27] B. Dong, N. Dyn, K. Hormann, Properties of dual pseudo-splines, applied and computational harmonic analysis, 29 (2010), pages 104-110.

[28] Y. Shen, S. Li, Wavelets and framelets from dual pseudo-splines, applied and computational harmonic analysis, 54 (2011), pages 1233-1242.

[29] Z. Chuang, J. Yang, A class of generalized pseudo-splines. Journal of Inequalities and Applications, 1 (2014), 359.